

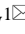

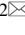


Geology, mineralogy and geochemistry of manganese ore deposits of the Um Bogma Formation, south-western Sinai, Egypt: Genesis implications

Shaimaa El-Shafei^{1*} , Fatma Ramadan¹ , Mohamed Essawy¹ ,
Ahmed Henaish¹ , Bassem Nabawy² 

¹ Zagazig University, Zagazig-Sharkia, Egypt

² National Research Center, Cairo, Egypt

*Corresponding author: e-mail shymaaelshafey11@gmail.com

Abstract

Purpose. This paper aims to understand the genesis and nature of the manganese ore deposits associated with the Ras Samra Member of the Um Bogma Formation in the southwest of Sinai.

Methods. Mineralogical and geochemical studies of 50 selected samples of manganese ores and host shale have been conducted. These samples have been taken from different sites representing the Ras Samra Member.

Findings. The dominant manganese minerals are pyrolusite and hausmannite. In most samples, helvite and hematite are noted in association with pyrolusite. In the investigated manganese ores, wide ranges of MnO (17.70-81.90 wt. %) and Fe₂O₃ (1.16-65.49 wt. %) concentrations are observed. Based on their Mn/Fe ratio, they can be classified into high-Mn ore content (76.94-6.46%), medium-Mn ore content (4.87-2.58%), and low-Mn ore content (1.51-0.30%).

Originality. The compositions of major and trace elements in Ras Samra manganese ores, together with their textures and mineralogical compositions, suggest an epigenetic hydrothermal contribution for high-Mn ores, as well as syngenetic sedimentary precipitation for medium- Mn and low-Mn ores. The epigenetic nature of the high-Mn samples may be related to a younger phase of hydrothermal activity associated with Tertiary basalt flows. Ore-bearing hypogene solutions, which penetrate the bedding planes, have impregnated and cemented non-diagenetic terrigenous sandstones and shale.

Practical implications. In contrast to low-Mn ores, high-Mn and medium-Mn ores of Um Bogma are preferable for obtaining a significant economic effect in the production of ferromanganese alloys. However, low-Mn ores need to be processed appropriately to achieve the desired quality in order to meet the present level of manganese demand in Egypt.

Keywords: manganese ores, Um-Bogma Formation, geochemistry, genesis, X-ray diffraction, X-ray fluorescence analysis

1. Introduction

The manganese ore deposits are diverse in occurrence, mineralogical and geochemical composition. They occur in a great diversity of host rocks such as carbonate, siliciclastic, volcanic and metamorphic rocks, as well as range in age throughout geologic history. These variations reflect differences in the formation processes and depositional environments, which in turn, are a response to changes in the land-ocean-atmosphere system over geologic time [1]. These deposits can be formed by one or more of four processes:

- 1) hydrogenetic precipitation from cold ambient seawater;
- 2) precipitation from hydrothermal fluids;
- 3) diagenetic precipitation from sediment pore waters;
- 4) replacement of rocks and sediments [2].

In addition, two mixed processes are assigned:

- 5) hydrogenetic and hydrothermal precipitation;
- 6) hydrogenetic and diagenetic precipitation.

These six processes can produce five morphological types of Fe-Mn deposits:

- 1) nodules and micronodules;
- 2) crusts and pavements;
- 3) cement and fracture-filling veins;
- 4) mounds and chimneys;
- 5) sediment-hosted strata-bound layers and lenses (Table 1).

The vast majority of land-based manganese resources occur as extensive layers of manganese-rich sedimentary rocks, some of which were formed as long as 2.5 billion years ago. These rocks were formed on the ancient seabed and became part of the continents during the tectonic processes of uplifting and continental accretion. They may have high enough manganese content to constitute the ores themselves, or they may be protores in which additional natural concentrating mechanisms have increased the manganese content enough to form commercial ores. A recent compilation of the chemical composition of the world's sedimentary manganese deposits indicates that the average manganese content is about 24%, and the iron content is 4.3% [3].

Received: 15 July 2022. Accepted: 3 September 2022. Available online: 30 September 2022

© 2022, S. El-Shafei, F. Ramadan, M. Essawy, A. Henaish, B. Nabawy
Mining of Mineral Deposits. ISSN 2415-3443 (Online) | ISSN 2415-3435 (Print)

This is an Open Access article distributed under the terms of the Creative Commons Attribution License (<http://creativecommons.org/licenses/by/4.0/>), which permits unrestricted reuse, distribution, and reproduction in any medium, provided the original work is properly cited.

Table 1. Forms of emplacement, processes of formation, and depositional/precipitation environment of the manganese ore deposits in the Um Bogma region

	Hydrogenetic	Hydrothermal	Diagenetic	Replacement	Hydrogenetic & hydrothermal	Hydrogenetic & diagenetic
Nodules	Abyssal plains, oceanic plateaus, seamounts ¹	Submerged calderas and fracture zones	Abyssal plains, oceanic plateaus	All areas (nodule nuclei)	Submerged calderas	Abyssal plains, oceanic plateaus ¹
Crusts	Midplate volcanic edifices ²	Active spreading axes, volcanic arcs, fracture zones, midplate edifices	–	Midplate edifices (crust substrate rock)	Active volcanic arcs, spreading axes, off axis seamounts, fracture zones	Abyssal hills
Sediment-hosted strata-bound layers and lenses	–	Active volcanic arcs, large midplate volcanic edifices, sediment-covered spreading-axes	Continental margins ³	Continental margins, volcanic arcs, midplate edifices	–	–
Cements	Midplate volcanic edifices ⁴	Active volcanic arcs, large midplate volcanic edifices ⁵	Midplate volcanic edifices ⁴	Volcanic arcs, midplate edifices	–	Midplate volcanic edifices ⁴
Mounds and chimneys	–	Back-arc basins, spreading centers, volcanic arcs	–	–	–	–

¹Less common on ridge, continental slopes, and shelves.

²Some seamounts, guyots, ridges, and plateaus are present.

³Fe and Mn carbonate lenses and concretions.

⁴Mostly fracture and vein fill, and cemented volcanic breccia.

⁵Mostly cemented breccia, sandstone and siltstone.

However, many of the currently mined manganese ores have been enriched in manganese to a greater extent by present land surface processes, although they were commonly formed in rocks that were already rich in manganese. These secondary enrichment types of deposits, or supergene deposits, are formed due to some chemical reactions occurring at a depth of tens of meters below the surface, with the redistribution of manganese on a local scale and the leaching of non-manganese components, which leads to residual manganese enrichment [4].

In Egypt, the major Fe-Mn mineralization occurs in two areas: Um Bogma on the south-western coast of Sinai and Elba in the southern part of the Eastern Desert. Additional small occurrences of ferromanganese ore deposits have been recorded in Mialik, Kalahin (Gebel Duwi), Wadi Abu Tarief, and Wadi Abu Shar.

The economic development of the Um Bogma region is mainly associated with the mining of manganese ores from Um Bogma Formation. The Um Bogma iron-manganese deposit is a large stratiform manganese-iron-oxide ore body occurring in carbonate rocks of marine origin. It occurs at different levels in the form of layers, sheets, lenses and pockets in the lower and middle members of the Um Bogma Formation. The ores consist of a heterogeneous mixture of iron and manganese oxides in various proportions [5].

Commercial mining of the Um Bogma ore began in 1918 and continued regularly until 1967. The total tonnage, shipped in 1955, was about of 3300000 tons. In 1956, about 240000 tons/annum of a shipping mixture containing 21.5% Mn, and 36% Fe was produced.

Despite numerous previous studies, the origin of the Mn-Fe ore deposits of Um Bogma is still controversial. The present study introduces new mineralogical and geochemical data on Mn-Fe ore deposits from the Ras Samra Member of

the Um Bogma Formation, along with the geochemical composition of host rocks. The results are discussed to understand the nature and genesis of these Mn-Fe ore deposits.

2. Geology and lithostratigraphy

The Um Bogma region is situated in the southwest of Sinai, 20 km east of the Gulf of Suez and 30 km southeast of Abu Zenima. It is bounded by 33°13'-33°31'E longitude and 28°48'-29°03'N latitude. It can be reached by an asphalt road that runs between the city of Abu Zenima and the tourist area of Sarabit El Khadim (Fig. 1) [6].

The Um Bogma region is mostly dominated by Paleozoic outcrops that rest on Precambrian basement rocks with some Triassic basalt flows (Fig. 1). Dolerite dykes associated with Tertiary volcanism (24.8 ± 1.5 m.y.) are also noted, penetrating the area in the NW-SE direction [7]. The Paleozoic outcrops in the Um Bogma region are subdivided into six rock units based on their lithological composition, fossil contents, and field relationships [8], [9]. These include from base to top: Sarabit El Khadim, Abu Hamata, Nasib, Adedia, Um Bogma, and Abu Thora formations (Fig. 2).

The entire Paleozoic succession rests unconformably on Precambrian basement rocks (Fig. 3a) and unconformably underlies the Triassic basalt sheets (Fig. 3b). The basement rocks comprise highly deformed gneisses, schists, and migmatites, which are intruded by high masses of old granitoids, younger pink granites, and post-granitic dykes [10]. Pink granites cover the highlands of the southern part of the study area.

The Sarabit El Khadim Formation (11-20 m thick) begins at the base with compact gravely sandstone interbedded with muddy brownish sandstone, which grades upward into fine-grained brownish and friable sandstone, followed by brownish laminated, fine-grained sandstone containing thin lenses of conglomerate and fine white gravel sandstone.

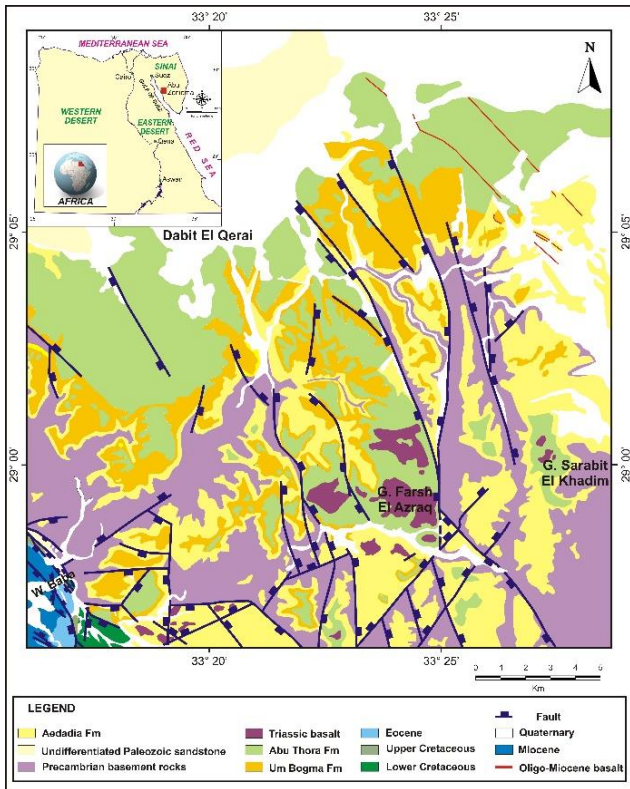


Figure 1. Geologic and structural map of the Um Bogma region [6]

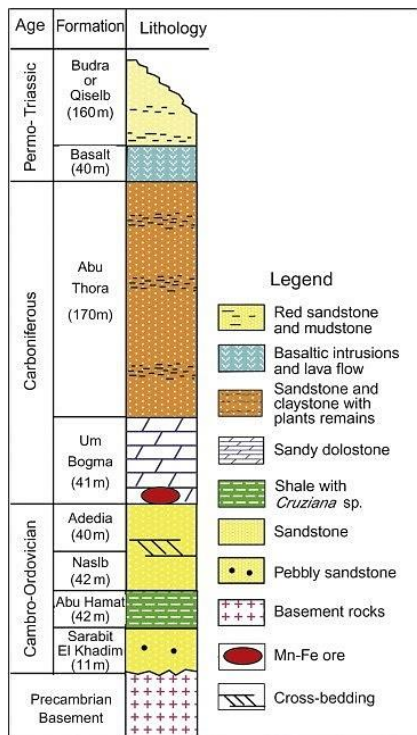


Figure 2. General lithostratigraphy of the Paleozoic succession in the Um Bogma area, west-central Sinai [8], [9]

The Abu Hamata Formation (40-62 m thick) is a fine-laminated, thin-bedded, yellowish-white to grey, fine-grained sandstone, stained with green copper carbonates, containing spots, patches and encrustations of manganese oxides. This sequence gradually changes into grey, fine laminated and fissile shaly sandstone, also stained with green copper carbonate minerals intruded along their fissile planes. The upper boundary is characterized by a gradual change from shale to sandstone.

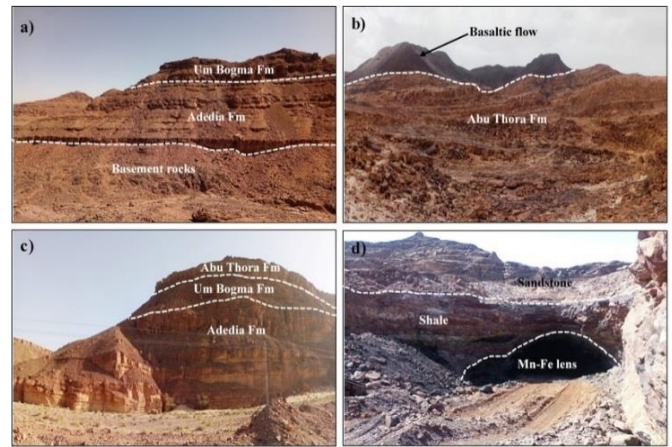


Figure 3. Photographs: (a) basement granitic rocks unconformably overlain by Paleozoic rocks; (b) basalt sheets unconformably overlain by the Paleozoic Abu Thora Formation; (c) general view of the Paleozoic succession in the Um Bogma area; (d) Mn-Fe lenses overlain by shale layer

The Adedia/Nasib Formation (30-82 m) is composed of sandstone and siltstone, which conformably overlie the Abu Hamata Formation. They are fine-grained with varying colors from white to yellow, massive, cross-laminated, with numerous sedimentary structures, such as tabular planar and trough cross-bedding.

The Um Bogma Formation (6-41 m) unconformably overlies the Adedia/Nasib Formation and is also unconformably overlain by the Abu Thora Formation (Fig. 3c). It is assumed that these unconformities are associated with tectonic instability, accompanied by block faults and changes in paleogeography during the Carboniferous period.

The Um Bogma Formation is composed of hard crystalline dolomite with some layers of limestone and marl. Based on lithology, it is subdivided into three members, from base to top these are: Ras Samra Member, El-Qor Member and Um Shebba Membe [11]-[14] (Fig. 4).

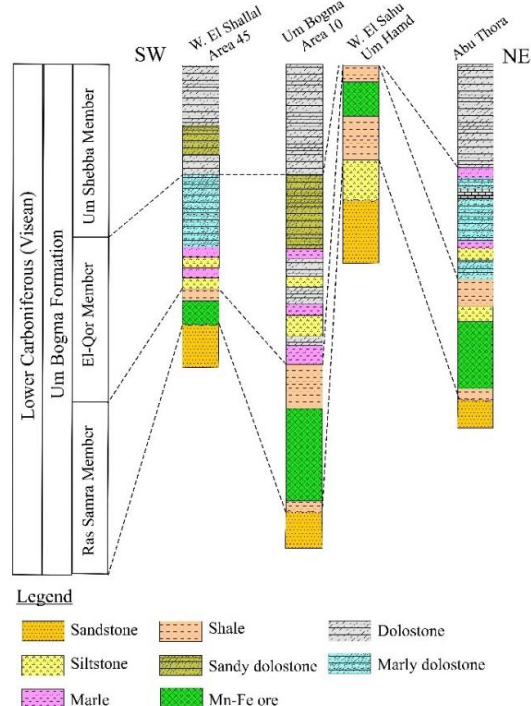


Figure 4. Lithostratigraphic subdivisions of the Um Bogma Formation [15]

The basal unit of the Um Bogma Formation, the Ras Samra Member, unconformably overlies the sandstone of the Adedia Formation. The thickness of this member differs from place to place, but its maximum section is 17 m at the entrance of Wadi Baba [16]. It is composed of hard, thick-bedded, pink-brown and coarse crystalline dolomite and shale containing manganese-iron concretions (Fig. 3d) and lenses, as well as secondary copper minerals that fill its fractures. Upwards, the middle El-Qor Member is composed of intercalations of yellowish marl and brown very hard massive marl dolomite and dolomitic limestone. The Upper Um Shebba Member conformably overlies middle marly dolomite; it is composed of hard thick dolostone with sandy dolostone in its middle parts.

The Abu Thora Formation (33-60 m, up to 170 m at its type section) is subdivided into three formations from base to top: El Hashash, Magharet El Maiah, and Abu Zarab [17]. This series is composed of shale, siltstone, sandstone, kaolin, clay, and carbonaceous shale. Triassic basalt sheets (60 m thick) usually overlie the Abu Thora Formation in the south-western parts of Sinai (Fig. 3b).

3. Structure

The Um Bogma region belongs to the Gulf of Suez tectonic province, where faults play the main role in its structural configuration. In the south and west of central Sinai, the Carboniferous rocks are primarily affected by normal faults, which are noted everywhere and vary greatly along the strike in the NNE-SSW direction, as well as in the NNW-SSE direction [18]. The prevailing trends of fault and joint systems in the west-central Sinai are the NNE and NNW directions [19].

The Um Bogma mining area is highly tectonized and affected by different faulting trends, namely N-S, NNW-SSE, NE-SW, and ENE-WSW [20], [21]. The N-S set acquires major faults of the greatest extent, extending up to 16 km. The faults of this trend are of the normal listric type [20]. This is almost the same trend as the eastern border fault of the Gulf of Suez rift. Some of the Carboniferous sedimentary rocks in the Um Bogma region are subjected to young rift tectonics in the Late Cenozoic, resulting in the formation of faults parallel to the Suez Rift, extending in the NNW-SSE and NW-SE directions of sinistral and dextral movements, respectively [22].

The Phanerozoic sedimentary cover and the underlying basement rocks of the Um Bogma region are dissected by a large number of rejuvenated strike-slips, as well as normal faults of different trends and conjugated patterns. Based on field relationships, [23] has identified the following tectonic phases in the studied area:

1. Post- and Pre-Cambrian tectonic phases are responsible for uplifting the Precambrian basement rocks prior to the deposition of fluvial deposits of the Sarabit El Khadim Formation.

2. The Syn-Sedimentary phase of the Intra-Cambrian fault resulted in the faulting of the Cambrian Sarabit El Khadim and Abu Hamata formations before the deposition of the subsequent Adedia Formation.

3. Post-Cambrian to Pre-Carboniferous faulting phase, leading to uplifting of the Cambrian succession prior to deposition of the Lower Carboniferous Um Bogma Formation. In some places, the Um Bogma Carboniferous carbonates rest directly on the Precambrian basement rocks or on very much reduced thickness of the Cambrian clastic rocks.

4. Intra-Lower Carboniferous fault phase, continuing the development of the lower dolostone ore member (Ras Samra

Member) of the Um Bogma Formation and the fossiliferous marly dolostone-siltstone member (El-Qor Member). This tectonic phase was probably responsible for uplifting the central part of the study area. During this tectonic phase, the uplifted areas are dominated by paleokarstification; while in the north-western corner of the Um Bogma region, Wadi Khaboba and Gebel Nukhul are dominated by continuous marine deposits.

5. The Post-Carboniferous fault phase is responsible for uplifting of the entire Paleozoic strata. Probably, the volcanic eruptions occurred during this tectonic phase.

6. A young fault phase is responsible for overlaying Paleozoic, Mesozoic, and Tertiary successions on each other and on Precambrian basement rocks.

4. Mineralization

Based on paleomagnetic studies [15], the Mn-Fe ore in the Um Bogma Formation and its host rocks are deposited during the Carboniferous. The manganese-iron deposits are more widespread in the Um Bogma region and are not limited to only three members of the Um Bogma Formation. It is noted at different stratigraphic levels of the area and usually has sharp contact with the host rocks. However, the main Mn mineralization is closely associated with Ras Samra Member of the Um Bogma Formation. In the south-eastern part of the Um Bogma area, where dolostones of the Um Bogma Formation are absent, the Mn-Fe horizon of deposits occupies the stratigraphic level of the Ras Samra Member and becomes a marker separating the overlying and underlying sandstone series. In this area, Mn-Fe ores are hosted in a thin ferruginous silty shale layer, conformable with lower and upper sandstones, with an average thickness of about 0.8 m (Fig. 3d). Most of the host shale is deposited in the Pre-Carboniferous period on an erosion surface existing between the Adedia Formation and the Um Bogma Formation [13], [24]. The change in the shale thickness is mainly attributed to its bending, contortion and soft flow under the overload pressures of the overlying massive dolostones and sandstone series.

The manganese ores of the Ras Samra Member are mainly concentrated in the form of stratiform lenticular bodies. They occur as a series of disconnected lenses about 2-3 m thick. This main ore horizon occurrence is exploited in a strip extending from the SW to the NE. Manganese lenses are vertically changed into more iron-rich ores or surrounded by iron ores. In many occurrences, manganese lenses are completely separated from the iron ore.

Upwards, manganese-iron deposits are noted at several stratigraphic levels within the El-Qor and the Um Shebba members. These ore bodies have more regular sheet-like shapes with a transition to thin detrital facies.

The vein-like type occurs in two places, namely Zobeir and Dakran areas. These ore deposits seem to be associated with fissures and faults. At Dakran, a fissure about 0.3 m wide cuts across the hard dolostones of the Ras Samra Member and is connected to the underlying ore pocket. The vein extends for about 4 m vertically. In the Zobeir area, the vein thickness is about 0.4 m, and it extends for about 3 m normal to the bedding planes. The host rock is a manganeseiferous mudstone replacing the lower dolostones of the Um Bogma Formation. Disseminated ore bodies sometimes fill the network of fractures in the pink dolostones of the Ras Samra Member.

5. Analytical techniques

More than 50 samples of Mn ores and host shale are collected from different sites, which represent the Ras Samra Member of the Um Bogma Formation in its type section in the southwest Sinai. The compositions of manganese ores are determined by the X-ray diffraction (XRD) technique using a (PW 3710 Based) diffractometer with Cu-K radiation ($\lambda = 1.78 \text{ \AA}$) at the Egyptian Mineral Resources Authority (EMRA) Central Laboratories. The main elemental analyzes of 39 rock samples of Mn ores and host shale are conducted in the Sinai manganese company (SMC) laboratories. Trace elements for 12 representative samples of high-Mn ores and

their host shale are determined using the X-ray fluorescence (XRF) technique in the Central Laboratories of Nuclear Materials Authority of Egypt. Besides, ten representative polished samples of Mn ores are examined using a reflected light microscope to recognize their diagnostic textures.

6. Results

6.1. Ore mineralogy

The XRD analyses of the studied samples reveal that the pyrolusite (MnO_2) and hausmannite (Mn_3O_4) are the dominant Mn-minerals (Fig. 5).

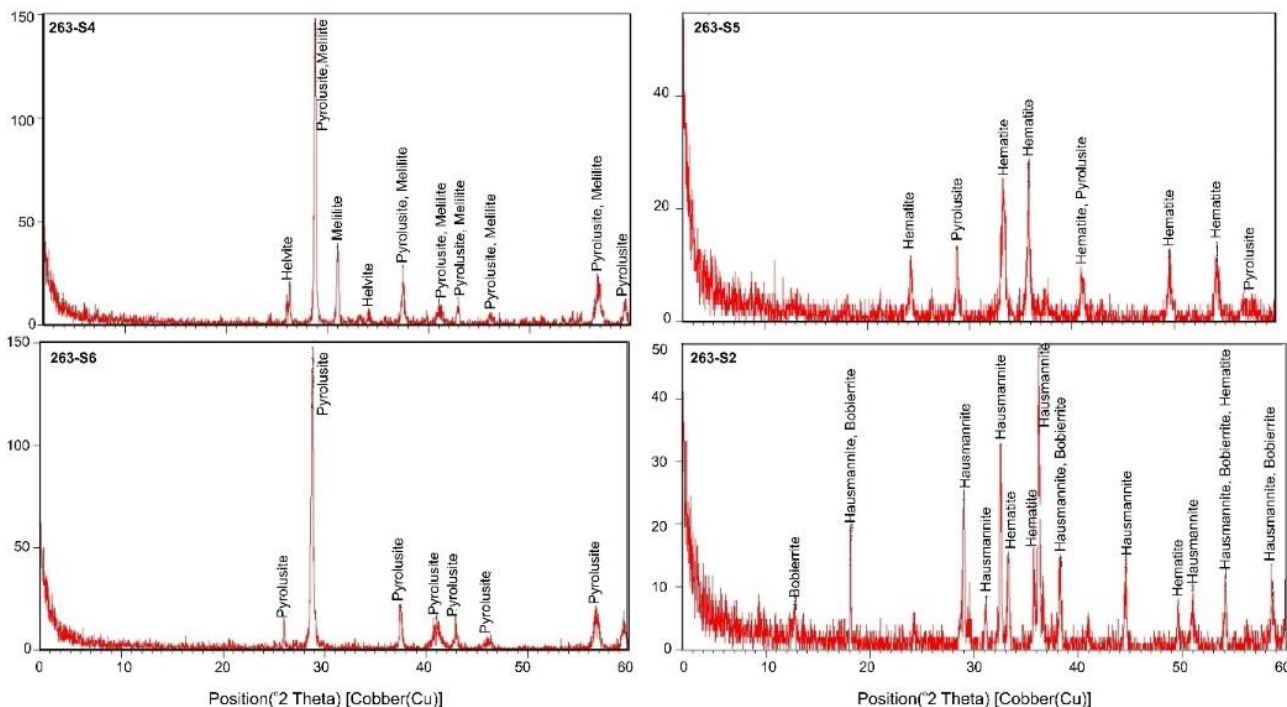


Figure 5. X-ray charts for the mineralogy of some Um Bogma Mn-ore samples

Minor amounts of helvite $[\text{Mn}_4(\text{BeSiO}_4)_3\cdot\text{S}]$ associated with pyrolusite are also recorded. Hematite is usually associated with pyrolusite and hausmannite in most of the studied ore samples. It can constitute the main component in some ore samples. Bobierite $[\text{Mg}_3(\text{PO}_4)_2\cdot 8\text{H}_2\text{O}]$ and melilite $[(\text{Ca},\text{Na})_2(\text{Al},\text{Mg},\text{Fe}^{2+})(\text{Al},\text{Si})\text{SiO}_7]$ are integral minor gangue minerals. Petrographic studies reveal that pyrolusite occurs as massive white to light brown fine-grained aggregates associated with gangue minerals. It usually has a characteristic colloform (crustiform bands) and radiant textures (Fig. 6a, b) sometimes including cavities. Late cross-cutting veinlets are also observed in most samples (Fig. 6b, c).

Hausmannite occurs as coarse-grained massive crystals from light to dark grey in color. It usually represents either the primary phase, later corroded by hematite (Fig. 6d), or the second phase, formed at the expense of hematite (Fig. 6e). In some samples, hausmannite exhibits spherical core-shell clusters (Fig. 6f).

6.2. Geochemistry

Chemical analyses of manganese ores and host shale are listed in Table 2.

According to [25], the studied manganese deposits can be chemically classified based on their Mn/Fe ratios into three types: high-Mn ore ($6 < \text{Mn/Fe}$), medium-Mn ore

($2 < \text{Mn/Fe} < 6$) and low-Mn ore ($\text{Mn/Fe} < 2$). The high-Mn Um Bogma ores are characterized by elevated Mn/Fe ratios up to 76.94 (Table 2) with an average value of 22. They have elevated values of Zn (average = 2828 ppm), V (average = 886 ppm), Pb (average = 774 ppm), Cu (average = 289 ppm), Co (average = 292 ppm), and Ni (average = 174 ppm). The medium-Mn and low-Mn ores have Mn/Fe ratios ranging from 2.2 to 4.4 and 0.3-1.5, respectively. Statistically, Mn % in the analyzed Mn-ores shows a strong negative correlation with Fe % (Fig. 7a).

On the other hand, it exhibits positive correlations with Pb % in the high-Mn ores (Fig. 7b). Samples with high, medium, and low manganese content are distinguished on the ternary plot ($10\cdot\text{MgO}-\text{Fe}_2\text{O}_3-\text{MnO}_2$) that has been introduced by [26] (Fig. 8a). The high-Mn samples predominantly plot in the field identified as terrestrial hydrothermal (I), while the low- and medium-Mn ores fall within and near the hydroge- netic marine zone (III and IV). However, all the present samples are outside the weathering zone (II, Fig. 8a). In Figure 8a, zones I, II, III, and IV are hydrothermal terrestrial, supergene terrestrial, hydrogenetic marine, and hydrogenetic freshwater zones, respectively.

The plot of Co + Ni values versus (Zn + V + Cu + Pb + Mo) values indicates that high-Mn-ores are located in the hydro- thermal zone (Fig. 8b).

Table 2. Major and trace element analyses of the manganese ores and the hosting shales

Area	Um Rinna					Zobeir mountain					Abu Zarab								
Ore type	High- Mn ore					High-Mn ore					Low-Mn ore			Medium-Mn ore					
S. No.	S1	S2	S3	S4	S5	S6	S7	S8	S9	S10	S11	S12	S13	S14	S15	S16	S17		
MnO	67.50	65.86	62.40	69.09	67.40	62.67	68.55	68.37	80.60	76.70	31.98	43.89	17.70	45.93	54.30	54.42	54.36		
Fe ₂ O ₃	5.71	6.01	10.70	8.72	7.87	8.58	6.86	7.48	1.16	1.84	46.48	37.75	65.35	33.82	23.34	20.95	19.59		
CaO	6.55	5.06	6.01	4.41	4.91	4.95	4.95	6.14	4.86	4.51	3.73	4.39	2.96	4.25	4.34	5.14	4.33		
MgO	1.93	1.70	2.35	1.41	1.51	1.56	1.40	1.88	1.46	1.32	1.11	1.48	1.08	1.25	1.30	1.69	1.31		
SiO ₂	6.40	4.16	6.31	7.14	4.42	7.11	5.89	4.22	4.94	5.80	4.70	4.95	3.07	9.06	10.33	9.84	8.72		
Al ₂ O ₃	6.59	7.81	6.56	5.28	6.29	7.05	4.85	5.16	5.31	4.76	4.47	4.46	3.09	4.21	4.39	5.59	5.58		
K ₂ O	0.53	0.62	0.45	0.36	0.41	0.41	0.41	0.39	0.41	0.38	0.33	0.45	0.24	0.35	0.34	0.38	0.42		
P ₂ O ₅	0.99	0.73	0.88	0.70	0.85	0.79	0.81	0.85	0.80	0.74	0.61	0.80	0.52	0.69	0.67	0.68	0.70		
Na ₂ O	0.56	0.50	0.56	0.43	0.52	0.53	0.53	0.44	0.45	0.42	0.34	0.43	0.27	0.43	0.46	0.46	0.39		
Total	96.76	92.44	96.21	97.54	94.17	93.66	94.25	94.93	99.99	96.47	93.76	98.60	94.29	100.0	99.48	99.15	95.40		
Mn %	52.28	51.01	48.33	53.51	52.19	48.54	53.09	52.95	62.42	59.40	24.77	33.99	13.71	36.35	42.06	42.15	42.10		
Fe %	3.99	4.20	7.48	6.10	5.50	6.00	4.80	5.23	0.81	1.29	32.51	26.40	45.71	24.00	16.32	14.65	13.70		
Mn/Fe	13.09	12.14	6.46	8.77	9.49	8.09	11.06	10.12	76.94	46.16	0.76	1.29	0.30	1.51	2.58	2.88	3.07		
Zn	4400	-	4176	-	-	-	-	-	2472	2856	-	-	-	-	-	-	-		
V	1635	-	n.d	-	-	-	-	-	100.7	319.0	-	-	-	-	-	-	-		
Cu	540.0	-	117.6	-	-	-	-	-	257.6	92.80	-	-	-	-	-	-	-		
Co	335.0	-	797.9	-	-	-	-	-	286.0	185.7	-	-	-	-	-	-	-		
Pb	340.5	-	275.5	-	-	-	-	-	1310	1106	-	-	-	-	-	-	-		
Ni	167.5	-	119.3	-	-	-	-	-	245.7	135.1	-	-	-	-	-	-	-		
Cr	n.d	-	n.d	-	-	-	-	-	n.d	n.d	-	-	-	-	-	-	-		
Mo	n.d	-	n.d	-	-	-	-	-	n.d	n.d	-	-	-	-	-	-	-		
Co/Zn	0.08	-	0.19	-	-	-	-	-	0.12	0.07	-	-	-	-	-	-	-		

Table 2. Continued

Area	Abu Hamata						No. 10						Abu Hamata				No.10			
Ore type	High-Mn ore						Medium-Mn ore		High-Mn ore		Medium-Mn ore		Low-Mn ore		Shale					
S. No.	S18	S19	S20	S21	S22	S23	S24	S25	S26	S27	S30	S31	S33	S29	S28	S32	H3	H4	H5	H6
MnO	69.88	75.96	81.90	72.52	80.70	66.54	66.09	65.02	67.02	71.74	54.92	62.99	55.08	42.02	21.10	24.23	0.27	0.54	1.05	0.22
Fe ₂ O ₃	5.15	4.29	1.95	5.69	1.33	9.37	15.02	18.30	7.58	6.01	13.79	16.16	27.31	42.90	65.49	60.06	15.00	14.70	19.40	15.60
CaO	6.84	5.05	3.87	5.23	4.50	4.22	4.38	4.21	5.16	5.95	4.92	6.64	5.65	4.62	3.19	3.38	3.32	3.48	5.10	8.48
MgO	1.45	1.41	1.06	1.48	1.26	1.29	1.58	1.50	1.47	1.66	2.81	1.90	1.89	1.36	0.90	0.97	2.00	2.57	1.63	3.62
SiO ₂	6.41	5.29	5.53	4.63	3.81	8.17	8.67	6.45	5.88	0.57	8.52	3.41	0.19	0.16	0.92	1.27	64.38	60.89	55.31	53.44
Al ₂ O ₃	5.31	5.37	3.87	5.87	4.84	4.94	2.27	2.50	5.71	6.11	5.93	5.42	4.88	4.33	3.15	4.95	13.72	16.98	17.02	18.13
K ₂ O	0.43	0.61	0.31	0.43	0.37	0.38	0.39	0.44	0.47	0.55	0.38	0.38	0.42	0.37	0.27	0.29	0.56	0.38	0.46	0.28
P ₂ O ₅	0.65	0.42	0.31	0.45	0.43	0.40	0.45	0.48	0.87	0.93	0.68	0.72	0.79	0.81	0.53	0.56	0.54	0.62	0.66	0.43
Na ₂ O	0.41	0.44	0.32	0.86	0.39	0.48	0.48	0.42	0.51	0.82	0.53	0.37	0.69	0.57	0.27	0.35	0.37	0.34	0.33	0.28
Total	96.52	98.84	99.13	97.18	97.62	95.79	99.34	99.33	94.66	94.35	92.46	97.98	96.90	97.14	95.83	96.05	100.2	100.5	101.0	100.5
Mn %	54.12	58.83	63.43	56.17	62.50	51.54	51.18	50.36	51.90	55.56	42.53	48.78	42.65	32.54	16.34	18.77	-	-	-	-
Fe %	3.60	3.00	1.36	3.98	0.93	6.55	10.50	12.80	5.30	4.20	9.64	11.30	19.10	30.01	45.81	42.01	-	-	-	-
Mn/Fe	15.03	19.61	46.51	14.11	67.19	7.87	4.87	3.93	9.79	13.23	4.41	4.32	2.23	1.08	0.36	0.45	-	-	-	-
Zn	-	-	1720	-	1344	-	-	-	-	-	-	-	-	-	-	-	336.0	285.6	538.4	403.2
V	-	-	1452	-	1812	-	-	-	-	-	-	-	-	-	-	-	306.2	762.5	310.5	185.4
Cu	-	-	352.0	-	376.8	-	-	-	-	-	-	-	-	-	-	-	58.2	460.0	77.6	88.0
Co	-	-	150.9	-	120.0	-	-	-	-	-	-	-	-	-	-	-	317.6	402.1	384.7	321.5
Pb	-	-	505.4	-	1106	-	-	-	-	-	-	-	-	-	-	-	137.7	142.6	165.9	109.6
Ni	-	-	247.3	-	128.0	-	-	-	-	-	-	-	-	-	-	-	89.3	106.7	154.8	150.9
Cr	-	-	n.d	-	n.d	-	-	-	-	-	-	-	-	-	-	-	534.5	436.6	1122	151.6
Mo	-	-	n.d	-	n.d	-	-	-	-	-	-	-	-	-	-	-	n.d	n.d	n.d	n.d
Co/Zn	-	-	0.09	-	0.09	-	-	-	-	-	-	-	-	-	-	-	-	-	-	-

The host shale samples show high concentrations of Cr (152-1122 ppm), Co (318-402 ppm), Zn (286-538 ppm), Pb (110-166 ppm), and Cu (58-460 ppm) (Table 2). Average values of high-manganese ores and their associated shales were normalized to average crustal values (North American Shale Composite, NASC) from [27] (Fig. 8c). The presentation of normalized major and trace elements (Sample/NASC) of the studied samples indicates a strong enrichment of high-manganese ores and host shale in some elements such as Mn, Zn, V, Co and Pb.

7. General discussion

7.1. Ore genesis

The Um Bogma manganese deposits were discovered by [28] and since then, they have been studied and described by many geologists. Two main theories have been put forward to explain its origin, these are the hydrothermal activity [5], [24], [29]-[32] and the sedimentary marine deposition [11], [15], [33]-[38].

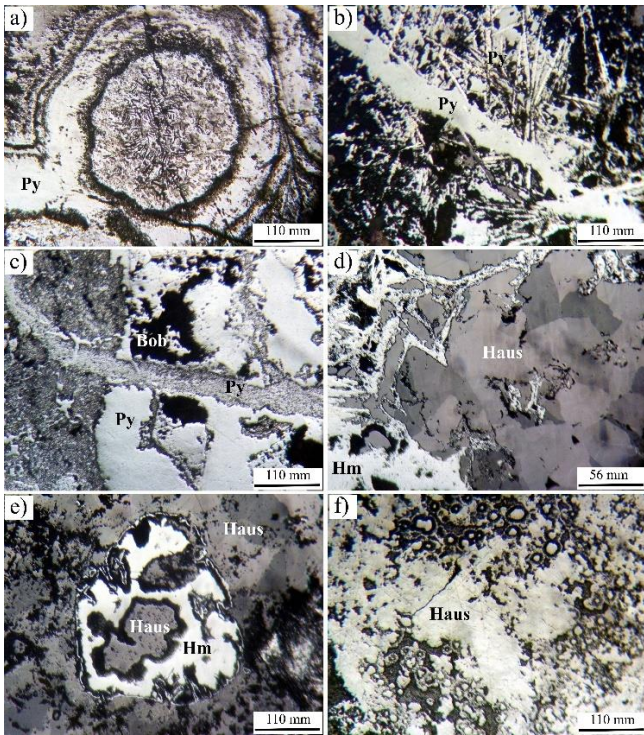


Figure 6. Photomicrographs: (a) colloform pyrolusite in high-Mn ore; (b) radiant pyrolusite intersected by pyrolusite veinlets in high-Mn ore; (c) different paragenetic phases of pyrolusite; (d) coarse-grained hausmannite replaced later by hematite; (e) hausmannite replaces the pre-existing hematite from cores and rims; (f) spherical hausmannite aggregates with core-shell structure. Note: Py is pyrolusite, Bob is Bobierrite, Haus is Hausmannite, and Hm is hematite

The former is based on two factors:

1) the close spatial relationship of Mn-Fe ore with the crosscutting dykes and faults, as well as the thickening of the ore body near these faults;

2) the presence of hausmannite and manganite as an indicator of hydrothermal activity. The latter, sedimentary origin, is attributed to the occurrence of penecontemporaneous dolomite, geochemical differentiation between Mn and Fe, stratigraphic control of ore bodies, and distribution of trace elements.

According to [39] the Mn/Fe ratio in hydrothermal deposits is higher than 10 or less than 0.1, while in hydrogenetic deposits it is almost equal to 1. Higher or lower values of Mn/Fe ratios are indicators of intense differentiation and segregation of these two elements in sedimentary environments and therefore reflect the hydrothermal origin of these deposits [5], [40]. The Mn/Fe ratios of the studied Mn-ores vary over a wide range (0.3-1.51 of average equals to 0.8 for low-Mn ore, 2.23-4.87 of average value of 3.5 for medium-Mn ore, and 8.09 to 77 of average value of 23 for high-Mn ore). Such wide ranges indicate that the mineralization is hydrogenetic in origin for both low- and medium-Mn samples and may be hydrothermal for high-Mn samples.

The Co/Zn ratio in the analyzed samples can be used to distinguish between the deposits of hydrothermal and hydrogenetic types [41], where the Co/Zn ratio of 0.15 indicates a deposit of hydrothermal type, while the ratio of 2.5 indicates the deposits of hydrogenetic type. The Co/Zn ratios of the studied high-Mn samples range from 0.01 to 0.19 with an average value of 0.09, which is close to the Co/Zn ratio for hydrothermal manganese deposits.

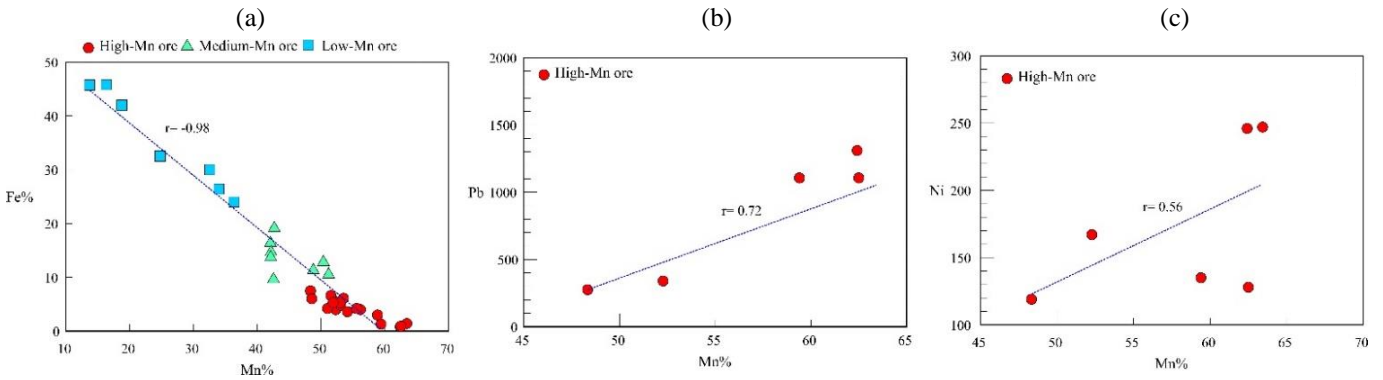


Figure 7. Variation diagrams for: (a) Mn % versus Fe % in Mn ores of the Ras Samra Member; (b) Mn % versus Pb in high-Mn ores of the Ras Samra Member; (c) Mn % versus Ni in high-Mn ores of the Ras Samra Member

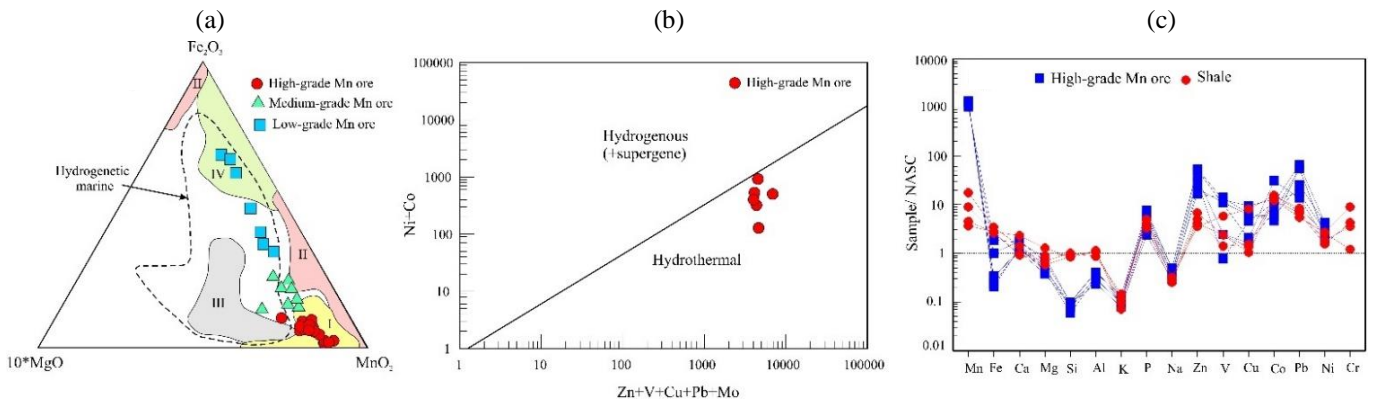


Figure 8. Classification diagrams: (a) (10·MgO-Fe₂O₃-MnO₂) ternary plot of Mn-ore deposits of the Ras Samra Member [26]; (b) Co + Ni versus (Cu + Mo + Pb + V + Zn) binary diagram for high-Mn ore deposits [42]; (c) NASC-normalized major and trace element patterns for high-Mn ore deposits and their host shales [27]

This is compatible with petrographic studies of high Mn-ores, which indicate that pyrolusite commonly displays primary hydrothermal colloform and radiant textures (Fig. 6a, b).

The presence of hausmannite (Fig. 6d-f) also suggests a hydrothermal origin for these manganese oxides [43]. Furthermore, the enrichment of the studied Mn-ores and host shale in Zn, Cu, V and Pb reflects the composition of the Mn-bearing hydrothermal fluids [43]-[45]. In addition, a strong negative correlation between the percentages of Mn and Fe ($r = -0.98$) suggests their precipitation under different environmental conditions, where fractionation occurs between these two elements during their formation [46]. Although the behavior of Fe and Mn is very similar, Mn is more mobile than Fe, especially in sedimentary environments [47]. Accordingly, Fe precipitates earlier than Mn, so they are differentiated and segregated from each other [5]. However, the regional occurrence of the scattered lenses of manganese and iron oxides in the same stratigraphic horizon of the Ras Samra Member of the Um Bogma Formation suggests contemporaneous formation of oxides in response to one common set of sedimentary conditions [48]. Moreover, the presence of manganese deposits in the form of well-defined lenses of considerable lateral continuity, parallel to bedding, suggests its formation as sediment. This interpretation is supported by high Co concentrations (120-798 ppm) in Mn-rich samples, which are considered an indicator of marine sedimentary environments [42]. This evidence points to a syngenetic sedimentary formation of the Ras Samra manganese deposits with a later epigenetic hydrothermal supply of most of its components followed by diagenetic recrystallization of the ore and gangue minerals [48]. This hydrothermal replacement and impregnation can be explained by the extensive activity of hypogenetic solutions associated with Tertiary basalt [49].

The elevated Ni, Cu, Zn and Pb content in the high-Mn ore suggests the presence of sulphides in the source area [50]. This is consistent with the presence of helvite in the Um Bogma Mn-ores. Subsequent leaching of these sulphides will affect the composition of manganese-bearing hydrothermal fluids [43].

7.2. Economic potentiality

The world reserves of manganese ores are about 630 million metric tons, and the annual global consumption is about 16 million metric tons. The rapid expansion in the world and Egyptian steel industry in recent years has increased the demand for the important ferromanganese alloy, necessitating an increase in the domestic reserves of these Mn-Fe ores. The total reserve of manganese ores in Um Bogma has been estimated at about 1.7 million tons [5].

Manganese is an essential metal for the production of most types of steel, where it increases its strength, toughness, hardness, and hardenability. It is added to steel or cast iron in the form of ferromanganese alloy [51]. Although the required amount of manganese to produce a ton of steel is small, ranging from 6 to 9 kg/ton, it is an indispensable component in the production of this fundamental material [52]. Manganese is also important in the production of cast iron [53]-[56]. Non-metallurgical applications of manganese include dyes, paints, battery cells, glass, and the textile industry. The manganese oxide has also been used for environmental purposes such as water and wastewater treatment [57].

The manganese oxides in manganese ores can be reduced to ferromanganese with carbon using heat supplied from carbon combustion in a Blast Furnace and electric power from Submerged Electric Arc Furnaces [58]. The reduction of manganese ore occurs in two successive stages. At the first stage, a gaseous reduction of iron and manganese oxides to FeO and MnO by CO is carried out in the solid state. At the second stage, direct reduction of MnO and FeO is performed by carbon to obtain metallic Mn and Fe. The completeness of the gaseous reduction affects directly the economics of the production process by increasing the efficiency of the carbonaceous reducer and decreasing the electric power consumption [51], [54]. It has been revealed that the reduction rates for high- and medium-Mn ores are higher compared to low-Mn ores. The authors attributed this to higher porosity and higher available oxygen compared to other low-Mn ore samples. The iron content of manganese ore decreases as its manganese content increases, and consequently oxygen available for its pre-reduction increases. The high oxygen available for the pre-reduction stage can lead to an important exothermic effect in the pre-reduction zone of the furnace, resulting in lower electric power consumption. Moreover, the higher ore porosity may be due to more complete reactions between manganese oxides and CO gas.

The present geochemical analyses indicate that surface Mn-deposits, associated with the Ras Samra Member of the Um Bogma Formation typically, consist of high-, medium-, and low-Mn ores. Accordingly, high- and medium- Mn ores can be economically promising deposits.

New investment in Um Bogma Mn-ores can be stimulated by upgrading the low-Mn ores using magnetic separation and acid bleaching as a method for beneficiation [53], [59]. It is also important to know the sub-surface nature of the ore to assess its potential [60]. The Ras Samra Mn-ores are described as stratiform deposits of variable thickness extending to great depths. Thus, deep vertical boreholes can be drilled in the ore body to assess its subsurface extension and potential [60].

The iron associated with Um Bogma manganese also is also of economic importance as a by-product of manganese extraction.

8. Conclusions

The main Mn-Fe ore deposits in the Um Bogma region primarily belong to the Ras Samra Member of the Um Bogma Formation. Mineralization occurs primarily in the form of stratiform lenticular ore bodies of lateral strike, enclosed in shale. In addition, ore bodies are present in the form of nodules, lenses, mounds, and chimneys at different lithostratigraphic levels of the Um Bogma section and overlying formations. Manganese ores generally have high-, medium-, and low-Mn concentrations with relatively high, medium, and low Mn/Fe ratios (6.46-76-94, 2.2-4.4, and 0.3-1.5, respectively).

The data on major and trace elements have revealed that high-manganese ores in the study area were probably formed from hydrothermal solutions, while medium- and low-Mn ores are predominantly of hydrogenetic-marine origin. Tertiary volcanic activity is a possible source of these hydrothermal Mn-ores. The high- and medium-Mn ore deposits in Ras Samra Member have potential as a raw material for the steel industry. On the other side, appropriate processing of low-Mn ores is necessary to achieve the desired quality, corresponding to the current level of manganese consumption in Egypt.

Acknowledgements

The authors are grateful to Lap management of Sinai manganese company (SMC), Egypt, for providing analytical facilities and to Professor Farouk Soliman for his suggestions for improving the manuscript. The authors also wish to thank the anonymous reviewers for critical revision and improving the manuscript, as well as Deputy Editor-in-Chief Vasyil Lozynskiy for editorial processing.

References

- [1] Nicholson, K., Hein, J.R., Bühn, B., & Dasgupta, S. (1997). *Manganese mineralization – Geochemistry and mineralogy of terrestrial and marine deposits*. Bath, United Kingdom: Geological Society Special Publication, 370 p.
- [2] Hein, J.R., Kochinsky, A., Halbach, P., Manheim, F.T., Bau, M., Kang, J.K., & Lubick, N. (1997). Iron and manganese oxide mineralization in the Pacific. *Manganese Mineralization: Geochemistry and Mineralogy of Terrestrial and Marine Deposits*, 119-123. <https://doi.org/10.1144/GSL.SP.1997.119.01.09>
- [3] Maynard, J.B. (2010). The chemistry of manganese ores through time: A signal of increasing diversity of Earth-surface environments. *Economic Geology*, 105(3), 535-552. <https://doi.org/10.2113/gsecongeo.105.3.535>
- [4] Varentsov, I.M. (1996). *Manganese ores of supergene zone: Geochemistry of formation*. Dordrecht, Netherlands: Kluwer Academic Publishers, 343 p. <https://doi.org/10.1007/978-94-017-2174-5>
- [5] Khalifa, I.H., & Seif, R.A. (2014). Geochemistry of manganese-iron ores at um Bogma area, west central Sinai, Egypt. *International Journal of Advanced Science and Technology*, (6), 1-6.
- [6] Moustafa, A.R. (2004). Geologic maps of the Eastern side of the Suez rift (western Sinai Peninsula), Egypt. *AAPG/Datapages, Inc. GIS Series* (Geologic Maps and Cross Sections in Digital Format on CD).
- [7] Steinitz, G., Bartov, Y., & Hunziker, J.C. (1978). K-Ar age determinations of some Miocene-Pliocene basalts in Israel: Their significance to the tectonics of the Rift Valley. *Geological Magazine*, 115(5), 329-340. <https://doi.org/10.1017/S0016756800037341>
- [8] Kora, M. (1984). *The Palaeozoic exposures of Um Bogma area, Sinai*. PhD Thesis. Mansoura, Egypt: Mansoura University, 280 p.
- [9] Wanas, H.A. (2011). The Lower Paleozoic rock units in Egypt: An overview. *Geoscience Frontiers*, 2(4), 491-507. <https://doi.org/10.1016/j.gsf.2011.06.004>
- [10] El-Aref, M.M., Abdel-Wahid, M., & Kabesh, M. (1988). On the geology of the basement rocks, East of Abu Zenima, west central Sinai. *Egyptian Journal of Geology*, 32(1-2), 1-25.
- [11] El Sharkawi, M.A., El Aref, M.M., & Abdel Motelib, A. (1990). Manganese deposits in a Carboniferous paleokarst profile, Um Bogma region, west-central Sinai, Egypt. *Mineralium Deposita*, (25), 34-43. <https://doi.org/10.1007/BF03326381>
- [12] Mansour, M (1994). *Sedimentology and radioactivity of Um Bogma Formation, West Central Sinai, Egypt*. MSc Thesis. Egypt: Suez Canal University, 157 p.
- [13] Kora, M., El Shahat, A., & Abu Shabana, M.A. (1994). Lithostratigraphy of the manganese-bearing Um Bogma Formation, west-central Sinai, Egypt. *Journal of African Earth Sciences*, 18(2), 15-162. [https://doi.org/10.1016/0899-5362\(94\)90027-2](https://doi.org/10.1016/0899-5362(94)90027-2)
- [14] Ashami, A.S. (2003). *Structural and lithologic controls of uranium and copper mineralization in Um Bogma environs, southwestern Sinai, Egypt*. PhD Thesis. Mansoura, Egypt: Mansoura University, 134p.
- [15] Elagami, N.L., Ibrahim, E.H., & Odah, H.H. (2000). Sedimentary origin of the Mn-Fe ore of Um Bogma, southwest Sinai: Geochemical and paleomagnetic evidence. *Economic Geology*, 95(3), 607-620. <https://doi.org/10.2113/95.3.607>
- [16] Kora, M. (1989). Lower Carboniferous (Viséan) fauna from Wadi Budra, west-central Sinai, Egypt. *Neues Jahrbuch für Geologie und Paläontologie-Monatshefte*, 523-538. <https://doi.org/10.1127/njgpm/1989/1989/523>
- [17] Soliman, M.S., & Abu El Fetouh, M.A. (1969). Petrology of Carboniferous sandstones in west central Sinai. *Journal of Geology of the United Arab Republic*, 13(2), 61-143.
- [18] Hilmy, M.E., & Mohsen, M. (1965). Secondary copper minerals from west central Sinai. *Egyptian Journal of Geology*, (9), 1-12.
- [19] Nabawy, B.S., & David, C. (2016). X-Ray CT scanning imaging for the Nubia sandstone as a tool for characterizing its capillary properties. *Geosciences Journal*, 20(5), 691-704. <https://doi.org/10.1007/s12303-015-0073-7>
- [20] El Aassy, I.E., El Rakaiby, M.L., & Botros, N.H. (1990). Geology and radioactivity of East Abu Zeneima Area, Sinai, Egypt. *Annals of the Geological Survey of Egypt*, (16), 285-288.
- [21] Elagami, N.L. (1996). *Geology and radioactivity studies on the Paleozoic rock units of Sinai Peninsula, Egypt*. PhD Thesis. Mansoura, Egypt: Mansoura University, 302 p.
- [22] Botros, N.H. (1995). The effect of rift tectonics on the mode of distribution of uranium bearing-sediments, Um Bogma area, West Central Sinai, Egypt. *Proceedings of Egypt Academic of Science*, (45), 193-204.
- [23] Aita, S.K. (1996). *Geological, mineralogical and geochemical studies on some radioactive anomalies of the Paleozoic sediments of Um Bogma area, west central Sinai, Egypt*. MSc Thesis. Cairo, Egypt: Cairo University, 262 p.
- [24] Weissbrod, T. (1969). The Palaeozoic of Israel and adjacent countries; Part II: The Palaeozoic outcrops in southwestern Sinai and their correlation with those of southern Israel. *Bulletin Geological Survey Israel*, (48), 1-32.
- [25] Dorokhin, I.V., Bogachero, E.N., Druzhiniv, A.V., Soboleviski, V.I., & Gorbunove, V. (1969). *Economic mineral deposits*. Moscow, Russian Federation: Higher school, 368 p.
- [26] Conly, A.G., Scott, S.D., & Bellon, H. (2011). Metalliferous manganese oxide mineralization associated with the Boleo Cu-Co-Zn district, Mexico. *Economic Geology*, 106(7), 1173-1196. <https://doi.org/10.2113/econgeo.106.7.1173>
- [27] Gromet, L.P., Dymek, R.F., Haskin, L.A., & Korotev, R.L. (1984). The "North American shale composite": Its compilation, major and trace element characteristics. *Geochim Cosmochim Acta*, (48), 2469-2482. [https://doi.org/10.1016/0016-7037\(84\)90298-9](https://doi.org/10.1016/0016-7037(84)90298-9)
- [28] Bauerman, H. (1869). Note on a geological reconnaissance made in Arabia Petraea in the Spring of 1868. *The Quarterly journal of the Geological Society of London*, 25(1-2), 17-38. <https://doi.org/10.1144/GSL.JGS.1869.025.01-02.15>
- [29] Attia, M.I. (1956). Manganese deposits of Egypt. In *Proceedings of the 20th International Geological Congress*, (II), 143-171.
- [30] Eisenlohr, V. (1965). Untersuchung der Manganerzlagert-itten, Um Bogma bei Abu Zeneima auf der Halbinsel Sinai. *Schriften der Dtsch Metallhiatten und Bergleut*, (15), 101-104.
- [31] Beyth, M. (1987). Mineralization related to rift systems: Examples from the Gulf of Suez and the Dead Sea Rift. *Tectonophysics*, (141), 191-197. [https://doi.org/10.1016/0040-1951\(87\)90185-5](https://doi.org/10.1016/0040-1951(87)90185-5)
- [32] Hassan, M.M., El-Ghawaby, M.A., Hilmy, M.E., Abu El-Izz, A.R., & Shehab, M. (1989). Iron manganese and copper mineralization in the Carboniferous sandstone, west central Sinai, Egypt. In *Proceedings of the First Conference on Geochemistry, Alexandria University*, 104-117.
- [33] El Shazly, E.M., Shukri, N.N., & Saleeb, G.S. (1963). Geological studies of Oleikat, Marahil and Um Sakran manganese-iron deposits, west central Sinai. *Journal of Geology*, 7(1), 1-27.
- [34] Faris, M.I., Youssef, M.I., & Kamel, O.A. (1963). Geology and origin of some vein manganese ores in Sinai: Cairo, Egypt. *Ain Shams Science Bulletin*, (9), 458-515.
- [35] Mart, J., & Sass, E. (1972). Geology and origin of the manganese ore of Um Bogma, Sinai. *Economic Geology*, 67(2), 145-155. <https://doi.org/10.2113/gsecongeo.67.2.145>
- [36] Magaritz, M., & Brenner, I.B. (1979). The geochemistry of a lenticular manganese-ore deposit (Um Bogma, Southern Sinai). *Mineralium Deposita*, 14(1), 1-13. <https://doi.org/10.1007/BF00201863>
- [37] Saleeb-Roufaiel, G.S., Yanni, N.N., & Arner, K.M. (1987). Contribution to the study of manganese-iron deposits at Um Bogma area, Sinai. *Earth Sciences Series*, (1), 98-107.
- [38] Zaghloul, Z.M., El Shahat, A., Kora, M., & Abu Shabana, M. (1995). Modes of occurrence, geochemistry and origin of the Mn-Fe deposits of Um Bogma, west central Sinai, Egypt. *Journal of Environmental Sciences*, (9), 29-59.
- [39] Rona, P.A. (1978). Criteria for recognition of hydrothermal mineral deposits in oceanic crust. *Economic Geology*, 73(2), 135-160. <https://doi.org/10.2113/gsecongeo.73.2.135>
- [40] Salem, I.A., El-Shibiny, N.H., & Abdel Monsef, M. (2016). Mineralogical and geochemical studies on manganese deposits at Abu Ghusun Area, South Eastern Desert, Egypt. *Journal of Geography and Earth Sciences*, 4(2), 51-74. <https://doi.org/10.15640/jges.v4n2a4>
- [41] Toth, J.R. (1980). Deposition of submarine crusts rich in manganese and iron. *Geological Society of America Bulletin*, 91(1), 44-54. [https://doi.org/10.1130/0016-7606\(1980\)91<44:DOSCRI>2.0.CO;2](https://doi.org/10.1130/0016-7606(1980)91<44:DOSCRI>2.0.CO;2)
- [42] Nicholson, K. (1992). Contrasting mineralogical-geochemical signatures of manganese oxides; guides to metallogenesis. *Economic Geology*, 87(5), 1253-1264. <https://doi.org/10.2113/gsecongeo.87.5.1253>
- [43] Nicholson, K. (1992). Genetic types of manganese oxide deposits in Scotland; indicators of paleo-ocean-spreading rate and a Devonian geochemical mobility boundary. *Economic Geology*, 87(5), 1301-1309. <https://doi.org/10.2113/gsecongeo.87.5.1301>
- [44] Nicholson, K. (1988). An ancient manganese-iron deposit of freshwater origin, Islay, Argyllshire. *Scottish Journal of Geology*, 24(2), 175-187. <https://doi.org/10.1144/sjg24020175>

- [45] Zantop, H. (1981). Trace elements in volcanogenic manganese oxides and iron oxides: the San Francisco manganese deposit, Jalisco, Mexico *Economic Geology*, 76(3), 545-555. <https://doi.org/10.2113/gsecongeo.76.3.545>
- [46] Krauskopf, K.B. (1957). Separation of manganese from iron in sedimentary processes. *Geochim Cosmochim Acta*, 12(1-2), 61-84. [https://doi.org/10.1016/0016-7037\(57\)90018-2](https://doi.org/10.1016/0016-7037(57)90018-2)
- [47] Simmonds, V., & Ghasemi, F. (2007). Investigation of manganese mineralization in Idahlu and Jokandy, southwest of Hashtrud, NW Iran. *BHM Bergund Hüttenmännische Monatshefte*, 152(8), 263-267. <https://doi.org/10.1007/s00501-007-0308-7>
- [48] Zantop, H. (1978). Geologic setting and genesis of iron oxides and manganese oxides in the San Francisco manganese deposit, Jalisco, Mexico. *Economic Geology*, 73(6), 1137-1149. <https://doi.org/10.2113/gsecongeo.73.6.1137>
- [49] Segev, A. (1984). Gibbsite mineralization and its genetic implication for the Um Bogma manganese deposit, southwestern Sinai. *Mineralium Deposita*, 19(1), 54-62. <https://doi.org/10.1007/BF00206597>
- [50] Hein, J.R., Schulz, M.S., Dunham, R.E., Stern, R.J., & Bloomer, S.H. (2008) Diffuse flow hydrothermal manganese mineralization along the active Mariana and southern Izu-Bonin arc system, western Pacific. *Journal of Geophysical Research*, (1130), 1-29. <https://doi.org/10.1029/2007JB005432>
- [51] Fahim, M.S., El Faramawy, H., Ahmed, A.M., Ghali, S.N., & Kandil, H.T. (2013). Characterization of Egyptian manganese ores for production of high carbon ferromanganese. *Journal of Minerals and Materials Characterization and Engineering*, 1(2), 68-74. <https://doi.org/10.4236/jmmce.2013.1.2013>
- [52] Binta, H. (2013). *Upgrading of Wasagu manganese ore to metallurgical grade concentrate*. MSc Thesis. Zaria, Nigeria: Ahmadu Bello University, 66 p.
- [53] Yaro, S.A. (1998). *Development of a process route for the beneficiation of Mallam Ayuba manganese deposit to ferromanganese feed grade*. PhD Thesis. Zaria, Nigeria: Ahmadu Bello University, 79 p.
- [54] Pochart, G., Joncourt, L., Touchard, N., & Perdon, C. (2007). Metallurgical benefit of reactive high grade ore in manganese alloys manufacturing. *World*, 800(1000), 1200.
- [55] Muriana, R.A., Muzenda, E., & Abubakre, O.K. (2014). Extraction and production kinetics of industrial – grade manganese sulphates crystal from manganese. *Journal of Engineering Research*, (19), 78-90.
- [56] Muriana, R.A., Muzenda, E., & Abubakre, O.K. (2014). Carbothermic reduction kinetics of Ka'oje (Nigeria) manganese ore. *Journal of Minerals and Materials Characterization and Engineering*, (2), 392-403. <https://doi.org/10.4236/jmmce.2014.25044>
- [57] Mücke, A. (2003). General and comparative considerations of whole-rock and mineral compositions of Precambrian iron-formations and their implications. *Neues Jahrbuch für Mineralogie-Abhandlungen*, 175-219. <https://doi.org/10.1127/0077-7757/2003/0179-0175>
- [58] Vanderstaay, E.C., Swinbourne, D.R., & Monteiro, M. (2004). A computational thermodynamics model of submerged arc electric furnace ferromanganese smelting. *Mineral Processing and Extractive Metallurgy*, 113(1), 38-44. <https://doi.org/10.1179/037195504225004706>
- [59] Binta, H., Yaro, S.A., Thomas, D.G., & Dodo, M.R. (2016). Beneficiation of low grade manganese ore from Wasagu, Kebbi State, Nigeria. *Journal of Materials Research*, 13(2), 1-8.
- [60] Mishra, P., Mohapatra, B.K., & Singh, P.P. (2006). Mode of occurrence and characteristics of Mn-ore bodies in iron ore group of rocks, North Orissa, India and its significance in resource evaluation. *Resource Geology*, 56(1), 55-64. <https://doi.org/10.1111/j.1751-3928.2006.tb00268.x>

Геологія, мінералогія та геохімія родовищ марганцевої руди формації Ум-Богма в південно-західному Синаї, Єгипет: можливі наслідки генезису

Ш. Ель-Шафей, Ф. Рамадан, М. Есаві, А. Хенайш, Б. Набаві

Мета. Вивчення генезису та природи родовищ марганцевої руди, пов'язаних із пачкою Рас-Самра формації Ум-Богма на південному заході Синаю на основі комплексу мінералого-геохімічних досліджень.

Методика. Проведено мінералого-геохімічні дослідження 50 відібраних проб марганцевих руд і вміщуючих сланців. Ці зразки були взяті з різних ділянок, що становлять пачку Рас Самра. Використані методи рентгенівської дифракції (XRD) та рентгенофлуоресцентного аналізу (XRF).

Результати. Встановлено, що домінуючими марганцевими мінералами є піролузит і гаусманніт. Виявлено, що у більшості проб відзначаються гелівіт та гематит у поєднанні з піролузитом. Встановлено, що у досліджуваних марганцевих рудах спостерігаються широкі діапазони концентрацій MnO (17.70-81.90 мас. %) і Fe₂O₃ (1.16-65.49 мас. %). Рекомендовано за співвідношенням Mn/Fe їх можна класифікувати на руди з високим вмістом марганцю (76.94-6.46%), руди із середнім вмістом марганцю (4.87-2.58%) і руди з низьким вмістом марганцю (1.51-0.30%).

Наукова новизна. Вперше виявлено, що склади основних елементів і мікроелементів у марганцевих рудах Рас-Самра разом із їх структурою та мінералогічним складом припускають епігенетичний гідротермальний внесок до руд з високим вмістом марганцю, а також сингенетичні осадові відкладення до руд із середнім і низьким вмістом марганцю.

Практична значимість. Для отримання значного економічного ефекту при виробництві феромарганцевих сплавів перевагу надають високомарганцевим і середньомарганцевим рудам Ум-Богми на відміну від низькомарганцевих руд. Проте руди з низьким вмістом марганцю необхідно обробляти відповідним чином для досягнення бажаної якості, щоб задовольнити поточний рівень попиту на марганець у Єгипті.

Ключові слова: марганцеві руди, формація Ум-Богма, геохімія, генезис, рентгенівська дифракція, рентгенофлуоресцентний аналіз